Localized Control of Proton Transfer through the D-Pathway in Cytochrome *c* Oxidase: Application of the Proton-Inventory Technique[†]

Martin Karpefors, Pia Ädelroth,[‡] and Peter Brzezinski*

Department of Biochemistry, The Arrhenius Laboratories for Natural Sciences, Stockholm University, SE-106 91 Stockholm, Sweden, and Department of Biochemistry and Biophysics, Göteborg University, P.O. Box 462, SE-405 30 Göteborg, Sweden

Received November 29, 1999; Revised Manuscript Received March 28, 2000

ABSTRACT: In the reaction cycle of cytochrome *c* oxidase from *Rhodobacter sphaeroides*, one of the steps that are coupled to proton pumping, the oxo-ferryl-to-oxidized transition (F → O), displays a large kinetic deuterium isotope effect of about 7. In this study we have investigated in detail the dependence of the kinetics of this reaction step [$k_{FO}(\chi)$] on the fraction (χ) D_2O in the enzyme solution (proton-inventory technique). According to a simplified version of the Gross−Butler equation, from the shape of the graph describing $k_{FO}(\chi)/k_{FO}(0)$, conclusions can be drawn concerning the number of protonatable sites involved in the rate-limiting proton-transfer reaction step. Even though the proton-transfer reaction during the F → O transition takes place over a distance of at least 30 Å and involves a large number of protonatable sites, the proton-inventory analysis displayed a linear dependence, which indicates that the entire deuterium isotope effect of 7 is associated with a single protonatable site. On the basis of experiments with site-directed mutants of cytochrome *c* oxidase, this localized proton-transfer rate control is proposed to be associated with glutamate (I-286) in the D-pathway. Consequently, the results indicate that proton transfer from the glutamate controls the rate of all events during the F → O reaction step. The proton-inventory analysis of the overall enzyme turnover reveals a nonlinear plot characteristic of at least two protonatable sites involved in the rate-limiting step in the transition state, which indicates that this step does not involve proton transfer through the same pathway (or through the same mechanism) as during the F → O transition.

Cytochromes aa_3 from *Rhodobacter sphaeroides* and from bovine heart belong to a family of proton-pumping terminal oxidases displaying a large degree of homology in the structures of subunits I−III. Both enzymes catalyze the oxidation of four cytochrome *c* molecules and the four-electron reduction of dioxygen to water. Electrons from cytochrome *c* are transferred sequentially from cytochrome *c* to Cu_A,[1] bound in subunit II, and then to heme *a* and the heme a_3−Cu_B binuclear center, all bound in subunit I. Molecular oxygen binds to the reduced heme a_3−Cu_B center, where it is reduced to water. The protons needed in this reaction are taken up specifically from the matrix in mitochondria or from the cytosol in the bacteria, defined as the input side. In addition, the free energy released in the O_2-reduction reaction is used to pump approximately one proton per electron from the input to the output side [for review, see (*1*)].

During catalysis, partially reduced oxygen intermediates are built-up to detectable concentrations, allowing observation of the transitions between these intermediates using the flow-flash technique [for review, see (*2*); for details of the reaction of *R. sphaeroides* with O_2, see (*3*)]. Upon reaction of the reduced enzyme with dioxygen, binding of O_2 to reduced heme a_3 is followed by oxidation of the two hemes forming the so-called peroxy intermediate (P) with a time constant of 30−50 μs. This reaction is then followed by formation of oxo-ferryl intermediate (F) with a time constant of ∼100 μs. Finally, the oxidized (O) enzyme is formed with a time constant of ∼1 ms (F → O transition). During enzyme turnover, proton pumping is coupled to the P → F and F → O transitions, and most likely also to reduction of the oxidized enzyme [see (*4*)].

With the detergent-solubilized enzyme, on average a net of four protons are taken up for each catalytic cycle. During reaction of the fully reduced enzyme with O_2, i.e., oxidation of the reduced enzyme, about two protons are taken up from solution (*3*), which implies that about two protons are taken up upon reduction of the oxidized enzyme [see also (*5*)]. In the flow-flash experiments outlined above, there is no proton uptake up to formation of the P intermediate, and the P → F and F → O transitions are associated with the uptake of about one proton each (*3*).

[†] Supported by grants from the Swedish Natural Science Research Council (NFR), The Swedish Council for Planning and Coordination of Research (FRN), and The Swedish Foundation for International Cooperation in Research and Higher Education (STINT).

* Correspondence should be addressed to this author at the Department of Biochemistry, The Arrhenius Laboratories for Natural Sciences, Stockholm University, SE-106 91 Stockholm, Sweden. FAX: (+46)-8-153679; phone: (+46)-8-163280; email: peterb@biokemi.su.se.

[‡] Present address: Department of Physics, University of California, San Diego, La Jolla, CA 92093-0354.

[1] Abbreviations: R, fully-reduced enzyme; A, ferrous-oxy intermediate; P, "peroxy" intermediate; F, oxo-ferryl intermediate; O, fully-oxidized enzyme; Cu_A, copper A; Cu_B, copper B; χ, mole fraction of D_2O; $k(\chi)$, rate measured in a fraction, χ, of D_2O; $DIE(\chi) = k(0)/k(\chi)$, deuterium isotope effect measured in a fraction, χ, of D_2O; ϕ_i^{TS} and ϕ_i^{RS}, isotopic fractionation factors of site *i* in the transition (TS) and reactant (RS) states, respectively; σ_i, ratio of the rate constants, $k_i(1)/k_i(0)$, at reacting site *i*; pH_{obs}, pH-meter reading; amino acid residue numbering, e.g., E(I-286) denotes glutamate-286 of subunit 1. **If not otherwise indicated, the amino acid numbering is based on the *R. sphaeroides* cytochrome *c* oxidase sequence.**

10.1021/bi992719t CCC: $19.00
Published on Web 05/19/2000

In the X-ray crystal structures of the bovine and *P. denitrificans* cytochrome *c* oxidases, two proton-transfer pathways have been identified leading from the proton-input side toward the binuclear center (*6*−*8*). One of these pathways is called the D-pathway because it "starts" with a highly conserved aspartate [D(I-132)], near the surface on the input side. The pathway consists of a number of polar/protonatable residues and water molecules, and it leads to another highly conserved residue, a glutamate [E(I-286)], which has been shown to play a central role in proton transfer to the binuclear center [for review, see (*9*)]. From E(I-286), the protons may be either transferred toward the binuclear center through a cavity which presumably contains several water molecules, or transferred toward the heme a_3 propionates, which are in contact with the proton-output side of the enzyme (*7*, *10*−*12*). Consequently, it has been proposed that E(I-286) may be a proton gate playing a central role in the regulation of the transfer rates of substrate protons, used for the O_2 chemistry, and of the pumped protons.

The D-pathway is the only pathway used during reaction of the fully reduced enzyme with dioxygen [for review, see (*9*)], and it is presumably used for the transfer of both substrate and pumped protons [the K-pathway is presumably used for proton uptake upon reduction of the oxidized enzyme and immediately after oxidation of the reduced enzyme; see (*4*, *9*, *13*)]. In the flow-flash experiment, the F → O transition, which involves the transfer of the fourth electron to the (three-electron-reduced) binuclear center, is one of the reaction steps coupled to proton pumping (*4*, *14*). We have previously shown that in the flow-flash experiment this electron transfer displays kinetic solvent deuterium isotope effects of ∼4 and ∼7 in the bovine and *R. sphaeroides* enzymes [(*15*, *16*); see also (*17*)], respectively.

In this study, we have extended the investigation of the kinetic deuterium isotope effect of the F → O transition by application of the proton-inventory technique (*18*−*20*). This technique has been used previously to provide information about the details of the rate-limiting steps of specific proton-transfer reactions, and it has been shown to be a valuable tool in investigations of the molecular mechanisms of enzymatic proton transfer (*18*, *19*, *21*−*23*).

Our results show that a plot of the F → O transition rate [$k_{FO}(\chi)/k_{FO}(0)$] as a function of the fraction D_2O (χ) is linear, which indicates that a single protonatable group is involved in the rate-limiting step in the transition state for the proton transfer through the D-pathway. Since the D-pathway spans over a distance of about 30 Å and involves a large number of protonatable residues and water molecules, the observation indicates that there is a single site in the pathway which controls the proton-transfer rate. Other experiments indicate that the most likely candidate for this site is glutamate (I-286) [see also (*15*)].

MATERIALS AND METHODS

Sample Preparation. The *R. sphaeroides* bacteria were grown aerobically in a 20 L fermentor. The enzyme was purified as described by Mitchell and Gennis [(*24*); see also (*3*)]. The bovine enzyme was prepared using the method of Brandt et al. (*25*). The concentration of cytochrome *c* oxidase was determined from the absorbance-difference spectrum of the dithionite-reduced minus ferricyanide-oxidized enzyme using an absorption coefficient $\epsilon^{604} - \epsilon^{630} = 24\ mM^{-1}\ cm^{-1}$ (*26*).

The oxidized enzyme was washed repetitively using Centricon-50 tubes (Amicon Inc.) with a H_2O or D_2O buffer consisting of 0.1 M Hepes, pH 7.5, 0.05% dodecyl-β-D-maltoside, and then diluted to the desired fraction of D_2O using different ratios of H_2O and D_2O (Sigma, 99.9%). After being washed, the solution was transferred to a modified anaerobic cuvette and made anaerobic by flushing pure N_2 that was saturated with "water" with the appropriate fraction of D_2O. The enzyme was reduced by sodium ascorbate at 5 mM using 5 μM PMS (phenazine methosulfate) as a mediator. To equilibrate the internal protonatable sites involved in proton transfer, the enzyme was "turned over" in a well-defined H_2O/D_2O mixture by addition of an air-saturated buffer solution, which contained a final concentration of O_2 that allowed about 10 full enzyme turnovers. After consumption of all oxygen, i.e., when the enzyme was again fully reduced (overnight incubation), the cuvette was flushed with "water"-saturated (cf. above) CO. All samples, also those containing 100% H_2O, were treated in the same way.

Measurements of the Kinetics of Electron and Proton Transfer. Measurements of absorbance changes associated with the reaction of the fully reduced enzyme with O_2 were done as described previously (*3*, *27*).

The experiments in H_2O, in D_2O, and in different mole fractions of D_2O, χ, were done at the same pH-meter reading (pH_{obs}). Due to the deuterium isotope effect on the pH-glass electrode, pL (the equivalent of pH in a mixture of H_2O and D_2O) is [see (*28*)]

$$pL \cong pH_{obs} + 0.076\chi^2 + 0.3314\chi \qquad (1)$$

i.e., in pure D_2O (at $\chi = 1$), $pL \equiv pD \cong pH_{obs} + 0.4$.

The deuterium isotope effect on the pK_a of a titratable group has a similar magnitude (i.e., $pK_{aD} \cong pK_{aH} + 0.4$). Assuming that this is also valid at intermediate fractions D_2O (χ), at the same pH-meter reading in different χ, the "protonation" state of the group is approximately the same. Assuming that the same applies to the protonatable groups within a protein, at the same pH-meter reading the "protonation" state of the protein should be the same in D_2O as in H_2O. However, it is important to note that the concentrations of protons in H_2O or deuterons in D_2O are different at the same pH-meter reading. Therefore, the experiments were done at a $pH_{obs} = 7.5$ at which the pH dependence of the F → O rate is small for both the *R. sphaeroides* (Ädelroth, unpublished) and bovine (*29*) enzymes. Thus, at this pH_{obs} the rate depends very little on the concentration of free protons/deuterons, and the rate is essentially insensitive to changes in the pK_a of protonatable groups.

Solutions with different mole fractions, χ, of D_2O were prepared by mixing the corresponding volume fractions D_2O/H_2O. By doing so, the error in χ is <1% since the larger molecular mass of D_2O (20.028) as compared to H_2O (18.015) is compensated for by the higher density of liquid D_2O (1.1044 g/cm^3 at 25 °C) as compared to liquid H_2O (0.99701 g/cm^3 at 25 °C).

Measurements of the Catalytic Activity. The catalytic activity of the enzyme was measured as the rate of oxidation

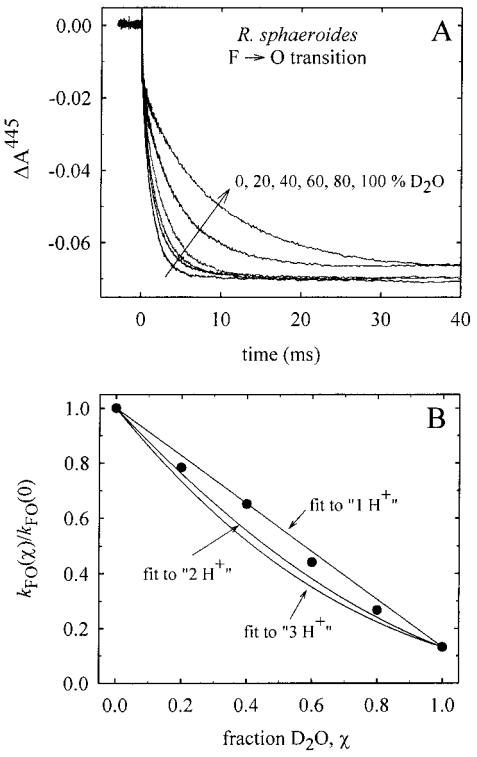

FIGURE 1: (A) Absorbance changes at 445 nm following flash photolysis of CO from the fully reduced *R. sphaeroides* cytochrome *c* oxidase in the presence of O_2. Prior to the experiment, the enzyme was incubated and turned over in a buffer containing a mixture of H_2O and D_2O with fractions of D_2O, χ, of 0, 0.2, 0.4, 0.6, 0.8, and 1.0. Conditions: 22 °C, 0.1 M Hepes, pH_{obs} 7.5, 0.05% dodecyl-β-D-maltoside, 0.3−0.7 μM reacting enzyme, 1 mM O_2. All traces have been scaled to the same enzyme concentration of 1 μM. (B) Ratio of the F → O transition rate [see (A)] measured with different solution fractions, χ, of D_2O, $k_{FO}(\chi)/k_{FO}(0)$, as a function of χ. The solid lines show fits of eq 4 ($\phi^{RS} = 1$) with $\{n = 1, \sigma = 0.14\}$ ("1 H^+"), $\{n = 2, \sigma_1 = \sigma_2 = 0.37\}$ ("2 H^+"), and $\{n = 3, \sigma_1 = \sigma_2 = \sigma_3 = 0.52\}$ ("3 H^+").

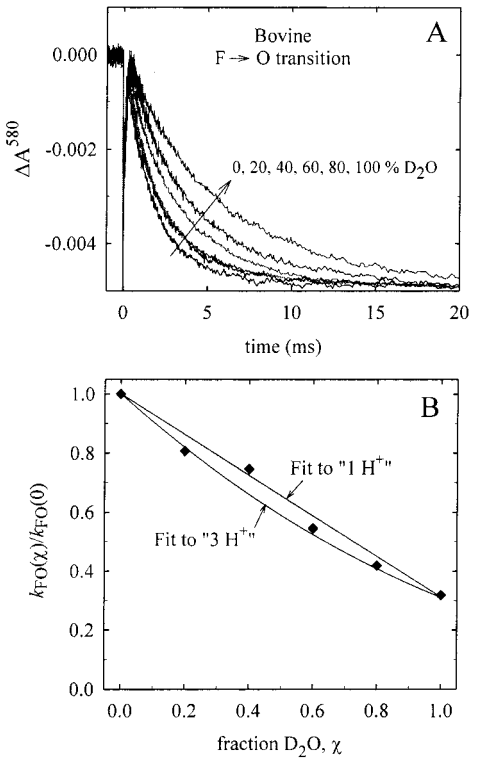

FIGURE 2: (A) Absorbance changes at 580 nm following flash photolysis of CO from the fully reduced bovine cytochrome *c* oxidase in the presence of O_2 at different fractions of D_2O as indicated in the figure. Conditions were the same as in Figure 1 except that the amount of reacting enzyme was 1.3−2.0 μM. All traces have been scaled to the same enzyme concentration of 1 μM. (B) Ratio of the F → O transition rate [see (A)] measured with different solution fractions, χ, of D_2O as a function of χ. The solid lines are fits of eq 4 ($\phi^{RS} = 1$) with $\{n = 1, \sigma = 0.29\}$ ("1 H^+") and $\{n = 3, \sigma_1 = \sigma_2 = \sigma_3 = 0.66\}$ ("3 H^+").

of reduced horse-heart cytochrome *c* (type VI, Sigma). Cytochrome *c* was reduced to more than 95% by hydrogen gas using platinum black (Aldrich, WI) as a catalyst (*30*) and stored under liquid nitrogen until use. The rate of oxidation was determined from the initial change in absorbance at 550 nm upon mixing the reduced cytochrome *c* with cytochrome *c* oxidase. The experiments were performed in 50 mM MES, pH_{obs} 6.5, with 0.05% dodecyl β-D-maltoside and different mole fractions of D_2O. The pH_{obs} of 6.5 (i.e., different from that used for the F → O transition) was chosen for the turnover−activity measurements because around pH_{obs} 6.5 the turnover activity displayed a small pH dependence (not shown).

RESULTS

Proton-Inventory Analysis of the F → O Transition. Figure 1A shows absorbance changes at 445 nm on the millisecond time scale following flash photolysis of CO from the fully reduced *Rhodobacter sphaeroides* cytochrome *c* oxidase in the presence of ~1 mM oxygen. The decrease in absorbance is associated with the decay of the oxo-ferryl (F) intermediate forming the oxidized (O) enzyme. The initial kinetic phases, discussed in the introduction [$\tau \leq 100$ μs; see also (*3*)], are not observed on this time scale. The experiments were done at different mole fractions D_2O (χ) and for each χ at five different wavelengths (410, 442, 445, 580, and 605 nm). The data obtained at all five wavelengths were fitted simultaneously with an exponential-decay function. In 100% H_2O, the rate constant was found to be 770 s^{-1}. As seen in Figure 1A, the F → O transition rate decreased with increasing fraction D_2O. The ratios of the F → O rates measured with different fractions D_2O and in pure H_2O [$k_{FO}(\chi)/k_{FO}(0)$], as a function of the fraction of D_2O (χ), are plotted in Figure 1B. The maximum deuterium isotope effect, measured in 100% D_2O [$k_{FO}(0)/k_{FO}(1)$], was found to be 7.1 ± 0.6 (SD of measurements with 3 samples).

The same experiments as those described above were also done with the bovine cytochrome *c* oxidase. With this enzyme, the absorbance changes associated with the F → O transition cannot be fitted with a single-exponential function at 445 nm (*3*), which complicates the data evaluation. Therefore, we measured the transients at 580 nm (Figure 2A), where these changes can more easily be fitted with a single-exponential function. As seen in Figure 2A, also with the bovine enzyme the rate decreases with increasing fraction D_2O. However, the maximum kinetic deuterium isotope effect was smaller, 4 ± 1.[2]

[2] The deuterium isotope effect with the bovine enzyme reported here is larger than that reported previously (~2.5) by Hallen and Nilsson (*31*). A deuterium isotope effect of 4.3 was observed after injection of one electron to the F state (formed by incubation in H_2O_2) of cytochrome *c* oxidase (*17*).

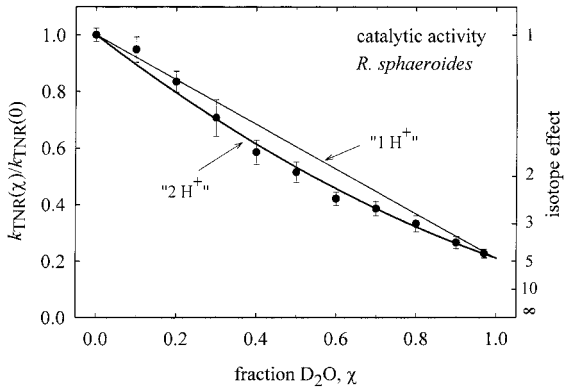

FIGURE 3: Ratios of the catalytic activity of the *R. sphaeroides* enzyme measured with different fractions D_2O and in 100% H_2O [$k_{TNR}(\chi)/k_{TNR}(0)$] are plotted as a function of the fraction D_2O. The solid lines are fits of eq 4 ($\phi^{RS} = 1$) with $\{n = 1, \sigma = 0.22\}$ (linear dependence, one site) and $\{n = 2, \sigma_1 = \sigma_2 = 0.47\}$ (two sites). Conditions: 22 °C, 0.05 M MES, pH_{obs} 6.5, 0.05% dodecyl-β-D-maltoside, 60 μM reduced cytochrome *c*. The enzyme concentration was 0.1 nM.

Proton-Inventory Analysis of the Catalytic Activity. The maximum turnover rates (O_2/s) of the *R. sphaeroides* and bovine enzymes were determined from the initial oxidation rates of horse heart cytochrome *c* at a pH-meter reading (see Materials and Methods) of 6.5 with different fractions of D_2O. A pH_{obs} of 6.5 was chosen because around this pH the activity is essentially independent of pH, which minimizes effects of pK_a changes of protein protonatable groups due to the isotopic exchange (see Materials and Methods). Figure 3 shows the dependence of the ratios of the turnover rates measured in different fractions D_2O and with 100% H_2O. With both the *R. sphaeroides* and bovine enzymes (not shown), the turnover rates decrease with increasing fraction D_2O. The maximum deuterium isotope effects, $DIE_{TNR}(1)$, were found to be 4.5 ± 0.8 and 2.7 ± 0.5 (SD of 6 and 3 measurements, respectively) for the *R. sphaeroides* and bovine enzymes, respectively, i.e., smaller than those for the F → O transition during single-turnover oxidation of the reduced enzymes (see also Table 1).

Temperature Dependence of the F → O Rate. The temperature dependence of the F → O transition rate was measured with the *R. sphaeroides* enzyme in 100% H_2O and 100% D_2O, respectively (not shown). The activation energies with H_2O and D_2O were 44 and 55 kJ/mol, respectively. Thus, the kinetic deuterium isotope effect displays an apparent activation energy of 11 kJ/mol.

DISCUSSION

A proton-transfer reaction involving a simple reorientation or breakage of a hydrogen bond leads to a deuterium isotope effect of $\sqrt{2}$ [see, e.g., (*32*)]. Reactions with larger deuterium isotope effects may involve several rate-limiting proton-transfer steps and/or "proton hopping" between two nearby protonatable sites (*28, 32, 33*). Alternatively, the proton transfer may be rate-limited by a structural rearrangement (see below). A useful approach for discriminating between the different possibilities is the use of the proton-inventory technique (*18, 19*). When using this technique, the ratio of the rate of a proton-transfer reaction measured at χ D_2O, $k(\chi)$, and in pure H_2O, $k(0)$, is assumed to depend on χ as shown in eq 2:

$$\frac{k(\chi)}{k(0)} = \frac{\prod_{i=1}^{n_{TS}}(1 - \chi + \chi\phi_i^{TS})}{\prod_{j=1}^{n_{RS}}(1 - \chi + \chi\phi_j^{RS})} \quad (2)$$

Here ϕ_i and ϕ_j are the isotopic fractionation factors, which are measures of the isotopic enrichment of sites *i* and *j*, in the protein relative to the deuterium preference of an average water molecule in the bulk solution, and TS and RS refer to the transition and reactant states, respectively. In other words, the properties of the reactant and transition states are treated independently.

A somewhat different formalism, which is independent of the mechanism of proton transfer and includes proton tunneling, was used by Krishtalik (*23*):

$$\frac{k(\chi)}{k(0)} = \frac{\prod_{i=1}^{n}(1 - \chi + \chi\sigma_i\phi_i^{RS})}{\prod_{j=1}^{n}(1 - \chi + \chi\phi_j^{RS})} \quad (3)$$

where σ_i is the ratio of the rate constants, $k_i(1)/k_i(0)$, at each reacting site. This gives formally the same expression as eq 2 above, but does not include a transition-state fractionation factor.

Experimentally, ϕ^{RS} for H_3O^+ is 0.69 (*34*). Theoretically, this value is determined by the difference in the zero-point energies of H_3O^+ and H_2O, ΔE_0, where E_0 is an essentially linear function of the O−H bond energy, i.e., of the pK_a of the donor (*20*). Since the pK_a of H_3O^+ is −1.7 and that of H_2O is 15.7, and $\phi^{RS} = 1$ for H_2O, the value of ϕ^{RS} for a group with a known pK_a can be estimated.

To discuss the general characteristics of the proton-inventory diagrams, we first assume for simplicity that $\phi_i^{RS} = 1$, which means that at equilibrium the protein groups involved in the rate-limiting proton-transfer step have the same isotopic enrichment as a water molecule in the bulk solution [(*18*); see also (*21, 35*)]. This assumption simplifies eq 3 to eq 4:

$$\frac{k(\chi)}{k(0)} = \prod_{i=1}^{n}(1 - \chi + \chi\sigma_i) \quad (4)$$

If the entire deuterium isotope effect is associated with a single site ($n = 1$), $k(\chi)/k(0)$ displays a linear dependence:

$$\frac{k(\chi)}{k(0)} = 1 - \chi + \chi\sigma \text{ for } n = 1 \quad (5)$$

where $\sigma = k(1)/k(0)$, i.e., the inverse of the deuterium isotope effect at 100% D_2O.

A nonlinear dependence arises if two or more proton sites contribute to the rate-limiting step of the proton-transfer

Table 1: Overall Turnover Activities and Rates of the F → O Transition in H_2O and D_2O, Respectively

	catalytic activity[a]			F → O transition		
enzyme	$k_{TNR}(0)$ (O_2/s)	$DIE_{TNR}(1)$	H^+ steps	$k_{F\rightarrow O}(0)$ (s^{-1})	$DIE_{F\rightarrow O}(1)$	H^+ steps
R. sphaeroides	300	4.5 ± 0.8	≥ 2	770	7.1 ± 0.6	1
bovine	125	2.7 ± 0.5	(*c*)	$\sim 1 \times 10^3$ s^{-1} [b]	4 ± 1	(*c*)

[a] In the flow-flash experiment, after completion of the reaction, four electrons have been transferred to O_2. Consequently, when comparing the activity of the enzyme with the rate of the slowest component of the flow-flash experiment (F → O), the O_2/s activity and not the e^-/s activity should be considered (*45*). For conditions, see figure legends. Note that the turnover activity and the F → O transition rate were measured at pH 6.5 and 7.5, respectively (see explanation in the text). The F → O transition rate is essentially pH independent below pH 7.5, while the turnover activity is ≤20% lower at pH 7.5 as compared to pH 6.5 [i.e., the difference between $k_{TNR}(0)$ and $k_{F\rightarrow O}(0)$ is greater at $pH_{obs} = 7.5$ as compared to $pH_{obs} = 6.5$]. [b] Major phase [see (*3*)]. [c] Due to the relatively small deuterium isotope effects, we were not able to determine the number of protonatable sites involved in the rate-limiting step of the proton-transfer reaction.

reaction; a rate-limiting proton-transfer step including two sites would result in a quadratic dependence, three sites in a cubic dependence, etc., while an infinite number of sites is characterized by an exponential dependence.

The experimental data in Figures 1B and 2B were fitted with eq 4 (solid lines). With the *R. sphaeroides* oxidase, the data were significantly better fitted using $n = 1$ (see eq 5) than with $n \geq 2$ (see Figure 1B). With the bovine enzyme, due to the experimental error and the smaller DIE(1) (see Figure 2B), we were not able to distinguish between $n = 1$ and $n \geq 2$.

For the *R. sphaeroides* enzyme, the linear fit of the $k_{FO}(\chi)/k_{FO}(0)$ graph indicates that there is a single, rate-limiting proton-transfer reaction in the transition state with $\sigma = 0.14 \pm 0.01$, i.e., a solvent deuterium isotope effect [DIE(1)] of about 7. The linear dependence may at first seem unexpected in light of the fact that during the F → O transition protons are transferred from the bulk solution to the binuclear center through the D-pathway, a distance of more than 30 Å, involving at least 10 water molecules (*11*, *12*) and protonatable amino acid side chains. As discussed below, this behavior is most likely a consequence of cytochrome *c* oxidase being a redox-driven proton pump.

A likely requirement for efficient function of a redox-driven proton pump is that internal electron-transfer rates are controlled by proton transfer (*1*, *2*, *36*), which is the case during the P → F and F → O transitions (*15*, *27*, *37*, *38*). In a recent study, we found that during the P → F ($\tau \cong 100$ μs) transition, proton transfer from a protonatable group in the D-pathway, presumably being E(I-286), to the binuclear center is rate-limiting for the overall P → F transition rate (*15*, *38*). The central role of E(I-286) in regulating the proton-transfer rate through the D-pathway has also been suggested earlier on the basis of theoretical calculations, which indicate that the side chain of this residue may adopt different positions: one position in which it is in contact with the proton-input side and one position in which it is in contact with the binuclear center or the proton-output side (*7*, *10*, *11*). Thus, the observation of a linear dependence of $k_{FO}(\chi)/k_{FO}(0)$ is likely to be due to the fact that a single group [E(I-286)] is involved in the rate-limiting step of the proton transfer through the D-pathway. The relatively large DIE(1) of ~7 indicates that the rate-limiting proton transfer involves proton hopping between two sites. As indicated above, the control of the proton-transfer rate by E(I-286) may be accomplished by a structural change of the E(I-286) side chain. Consequently, an alternative interpretation of the linear proton-inventory plot of the F → O transition is that the rate-determining step is not the proton transfer itself, but rather the structural change of the side chain of E(I-286).

The difference in the apparent activation energies of the F → O transition in H_2O and D_2O, respectively, of 11 kJ/mol, gives a ratio of the Arrhenius factors of ~80:

$$\frac{k(0)}{k(1)} = \frac{A_H e^{-E_{aH}/RT}}{A_D e^{-E_{aD}/RT}} \cong 80\frac{A_H}{A_D} \qquad (6)$$

To obtain a DIE(1) of ~7, $A_D \cong 12A_H$; i.e., the preexponential factor is larger for deuterium than for protium. Because the tunneling probability of deuterium should be smaller than that of protium, the larger A_D than A_H implies that the mechanism does not involve a simple proton tunneling between two spatially fixed sites. This situation can be explained in terms of an approach of the proton donor and acceptor to obtain an optimum tunneling distance [for review, see (*20*)]. As the tunneling of deuterium is less likely than that of protium, the deuterium must approach closer to the acceptor and hence the larger apparent activation energy for deuterium (in addition, the optimum distance may also be temperature dependent). In conclusion, collectively, these results indicate that the side chain of E(I-286) must approach the proton acceptor in order to facilitate the proton transfer (Figure 4).

Assuming that E(I-286) is the proton-donating group in the rate-limiting proton transfer during the F → O transition, the value ϕ^{RS} can be estimated from the pK_a of the group, i.e., from the pK_a determined from the pH dependence of the F → O transition rate. For the *R. sphaeroides* enzyme, this pK_a was found to be ~8.5 (Katsonouri and Aagaard, unpublished results), which implies that $\phi^{RS} \cong 0.87$ [interpolated value between 0.69 ($pK_a = -1.7$) and 1 ($pK_a = 15.7$); see above]. The use of $\phi^{RS} \cong 0.87$ in eq 3 does not greatly change the shape of the fitted curve (see Figure 1).

At all fractions D_2O, χ, the kinetic phase associated with the F → O transition in the *R. sphaeroides* enzyme could be satisfactorily fitted with a single-exponential phase (the residuals, i.e., the difference between the experimental data and the fit, were <5% of the total absorbance change), but not with a biexponential function with the rates fixed at values corresponding to those in pure H_2O and pure D_2O, respectively. The latter case reflects a situation in which there are two enzyme populations, one in which the protonatable site involved in the rate-limiting step (see below) is deuterated and one in which it is protonated. This result indicates that at the different fractions D_2O, during the F → O transition, on the time scale of the measurements, the

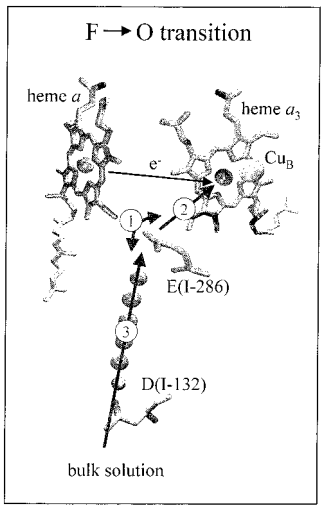

FIGURE 4: Reaction scheme summarizing the experimental results for the F → O reaction step. The observed F → O rate is determined by a single rate-limiting proton-transfer step that involves a conformational change of the E(I-286) side chain (step 1). Proton transfer from E(I-286) to the binuclear center (step 2) is followed by rapid re-protonation of E(I-286) from the bulk solution (step 3). The spheres are water molecules in the D-pathway (arbitrarily positioned). Coordinates are from (*8*). The illustration was made using the Visual Molecular Dynamic Software (Theoretical Biophysics Group, Beckman Institute for Advanced Science and Technology, University of Illinois at Urbana−Champaign).

protonatable site was in rapid (i.e., much faster than the F → O transition) equilibrium with a pool of "water" molecules reflecting the same fraction D_2O as in the bulk solution (either the bulk solution itself or water molecules within the protein, around the protonatable site).

A relatively large DIE(1) was also found for the M-intermediate formation step in the photocycle of bacteriorhodopsin (*35*, *39*). In this step, which involves proton transfer from the Schiff base to Asp85 in the extracellular region, curved proton-inventory plots were found (*35*), indicating at least two protonatable sites involved in the reaction.

The proton-inventory analysis of the overall turnover rate of the *R. sphaeroides* enzyme shows that the data were significantly better described using $n \geq 2$ than $n = 1$ in eq 4 (see Figure 3). For example, with $n = 2$, i.e., two sites involved in the rate-limiting proton-transfer step, eq 4 simplifies to

$$\frac{k(\chi)}{k(0)} = (1 - \chi + \chi\sigma_1)(1 - \chi + \chi\sigma_2) \qquad (7)$$

A fit of the data with the *R. sphaeroides* enzyme in Figure 3 using eq 7 with $\sigma_1 = \sigma_2 = \sigma$ gives $\sigma = 0.47$; i.e., for each site, the "deuterium-isotope effect" is ∼2.2 and the total deuterium-isotope effect, DIE(1), is $(0.47 \cdot 0.47)^{-1} \cong 4.5$. With the bovine enzyme, we were not able to determine the value of *n* due to the smaller DIE(1).

The rate of the slowest electron-transfer step during single-turnover oxidation of the reduced enzyme (F → O) was faster than the overall turnover rate in both the *R. sphaeroides* and bovine enzymes (see Table 1), which shows that the rate-limiting step for the overall turnover reaction is not the F → O transition [this conclusion is different from our earlier interpretation of the data (*3*); see footnote *a* in Table 1]. In addition, the smaller DIE(1) of the turnover activity as compared to that of the F → O transition and the different shapes of the proton-inventory curves with the *R. sphaeroides* enzyme indicate that the rate-limiting step of the turnover does not involve proton transfer through the D-pathway or involves a different mechanism.

With both enzymes, we have previously observed a slower proton-uptake phase with a time constant of ∼5 ms (*3*), after oxidation of the reduced enzyme. In addition, electrogenic events with a similar time constant were observed (*40*, *41*). Since the rate constant of this slower component compares to the overall turnover rate of the *R. sphaeroides* cytochrome *c* oxidase (see Table 1), for this enzyme, this kinetic phase may be associated with events that are rate-limiting for the overall cycle. In a recent study, Verkhovsky et al. (*4*) suggested that after oxidation of the fully reduced cytochrome *c* oxidase, the enzyme is in a higher energy state as compared to the resting enzyme. The reduction of the enzyme in this state results in pumping of protons, and this step may be rate-limiting for the overall enzyme turnover [see also (*2*, *40*, *42*)]. The reductive phase of the cytochrome *c* oxidase reaction cycle involves proton uptake through the K-pathway (*43*, *44*), and it is likely that the same pathway is also used for proton uptake during the second reduction cycle following immediately after oxidation of reduced enzyme. If this is the case, the nonlinear proton-inventory curve may reflect proton transfer through the K-pathway.

CONCLUSIONS

In conclusion, the results with the *R. sphaeroides* cytochrome *c* oxidase presented in this paper show that the F → O reaction step, one of the transitions associated with proton pumping, displays a solvent kinetic deuterium isotope effect of ∼7 (in 100% D_2O). The rate-limiting step of the F → O transition is proton transfer through the D-pathway, and the entire solvent-isotope effect is attributed to a single protonatable site in this pathway, E(I-286) (Figure 4).

ACKNOWLEDGMENT

We thank Prof. Lev Krishtalik (Russian Academy of Sciences) for critically reading the manuscript and for his extremely helpful comments. We are also indebted to Dr. Dmitry Zaslavsky for valuable discussions.

REFERENCES

1. Ferguson-Miller, S., and Babcock, G. T. (1996) *Chem. Rev. 96*, 2889−2907.
2. Babcock, G. T., and Wikström, M. (1992) *Nature 356*, 301−309.
3. Ädelroth, P., Ek, M., and Brzezinski, P. (1998) *Biochim. Biophys. Acta 1367*, 107−117.
4. Verkhovsky, M. I., Jasaitis, A., Verkhovskaya, M. L., Morgan, J. E., and Wikström, M. (1999) *Nature 400*, 480−483.
5. Mitchell, R., and Rich, P. R. (1994) *Biochim. Biophys. Acta 1186*, 19−26.
6. Fetter, J. R., Qian, J., Shapleigh, J., Thomas, J. W., García-Horsman, A., Schmidt, E., Hosler, J., Babcock, G. T., Gennis, R. B., and Ferguson-Miller, S. (1995) *Proc. Natl. Acad. Sci. U.S.A. 92*, 1604−1608.
7. Iwata, S., Ostermeier, C., Ludwig, B., and Michel, H. (1995) *Nature 376*, 660−669.
8. Tsukihara, T., Aoyama, H., Yamashita, E., Tomizaki, T., Yamaguchi, H., Shinzawa-Itoh, K., Nakashima, R., Yaono, R., and Yoshikawa, S. (1996) *Science 272*, 1136−1144.

9. Brzezinski, P., and Ädelroth, P. (1998) *J. Bioenerg. Biomembr. 30*, 99−107.
10. Puustinen, A., and Wikström, M. (1999) *Proc. Natl. Acad. Sci. U.S.A. 96*, 35−37.
11. Hofacker, I., and Schulten, K. (1998) *Proteins: Struct., Funct., Genet. 30*, 100−107.
12. Riistama, S., Hummer, G., Puustinen, A., Dyer, R. B., Woodruff, W. H., and Wikström, M. (1997) *FEBS Lett. 414*, 275−280.
13. Brzezinski, P., and Ädelroth, P. (1998) *Acta Physiol. Scand. 163*, 7−16.
14. Oliveberg, M., Hallén, S., and Nilsson, T. (1991) *Biochemistry 30*, 436−440.
15. Karpefors, M., Ädelroth, P., Aagaard, A., Smirnova, I. A., and Brzezinski, P. (1999) *Isr. J. Chem. 39*, 427−437.
16. Karpefors, M., Ädelroth, P., and Brzezinski, P. (2000) *Biochemistry 39*, 5045−5050.
17. Zaslavsky, D., Sadoski, R. C., Wang, K. F., Durham, B., Gennis, R. B., and Millett, F. (1998) *Biochemistry 37*, 14910−14916.
18. Venkatasubban, K. S., and Schowen, R. L. (1984) *Crit. Rev. Biochem. 17*, 1−44.
19. Schowen, K. B., Limbach, H.-H., Denisov, G. S., and Schowen, R. L. (2000) *Biochim. Biophys. Acta* (in press).
20. Krishtalik, L. I. (2000) *Biochim. Biophys. Acta* (in press).
21. Vidakovic, M., Sligar, S. G., Li, H. Y., and Poulos, T. L. (1998) *Biochemistry 37*, 9211−9219.
22. Venkatasubban, K. S., and Silverman, D. N. (1980) *Biochemistry 19*, 4984−4989.
23. Krishtalik, L. I. (1993) *Mendeleev Commun.*, 66−67.
24. Mitchell, D. M., and Gennis, R. B. (1995) *FEBS Lett. 368*, 148−150.
25. Brandt, U., Schägger, H., and von Jagow, G. (1989) *Eur. J. Biochem. 182*, 705−711.
26. Vanneste, W. H. (1966) *Biochemistry 5*, 838−848.
27. Ädelroth, P., Svensson Ek, M., Mitchell, D. M., Gennis, R. B., and Brzezinski, P. (1997) *Biochemistry 36*, 13824−13829.
28. Schowen, K. B., and Schowen, R. L. (1982) *Methods Enzymol. 87*, 551−606.
29. Oliveberg, M., Brzezinski, P., and Malmström, B. G. (1989) *Biochim. Biophys. Acta 977*, 322−328.
30. Rosen, P., and Pecht, I. (1976) *Biochemistry 15*, 775−786.
31. Hallén, S., and Nilsson, T. (1992) *Biochemistry 31*, 11853−11859.
32. Agmon, N. (1995) *Chem. Phys. Lett. 244*, 456−462.
33. Bell, R. P. (1980) in *The tunnel effect in chemistry*, pp 77−115, Chapman and Hall, New York.
34. Albery, W. J. (1967) in *Progress in Reaction Kinetics* (Porter, G., Ed.) Vol. 4, p 353, Pergamon, Oxford.
35. Brown, L. S., Needleman, R., and Lanyi, J. K. (2000) *Biochemistry 39*, 938−945.
36. Babcock, G. T., Floris, R., Nilsson, T., Pressler, M., Varotsis, C., and Vollenbroek, E. (1996) *Inorg. Chim. Acta 243*, 345−353.
37. Karpefors, M., Ädelroth, P., Zhen, Y. J., Ferguson-Miller, S., and Brzezinski, P. (1998) *Proc. Natl. Acad. Sci. U.S.A. 95*, 13606−13611.
38. Smirnova, I. A., Ädelroth, P., Gennis, R. B., and Brzezinski, P. (1999) *Biochemistry 38*, 6826−6833.
39. Le Coutre, J., and Gerwert, K. (1996) *FEBS Lett. 398*, 333−336.
40. Konstantinov, A. A. (1998) *J. Bioenerg. Biomembr. 30*, 121−130.
41. Jasaitis, A., Verkhovsky, M. I., Morgan, J. E., Verkhovskaya, M. L., and Wikström, M. (1999) *Biochemistry 38*, 2697−2706.
42. Verkhovsky, M. I., Morgan, J. E., and Wikström, M. (1995) *Biochemistry 34*, 7483−7491.
43. Vygodina, T. V., Pecoraro, C., Mitchell, D., Gennis, R., and Konstantinov, A. A. (1998) *Biochemistry 37*, 3053−3061.
44. Ädelroth, P., Gennis, R. B., and Brzezinski, P. (1998) *Biochemistry 37*, 2470−2476.
45. Zaslavsky, D., and Gennis, R. B. (2000) *Biochim. Biophys. Acta* (in press).

BI992719T